Joint Antenna and Channel Modelling for Communication in Metallic Kitchen Environments

Brecht De Beelde, Nico Podevijn, David Plets, Emmeric Tanghe, Luc Martens, Wout Joseph

INTEC/WAVES, IMEC, Ghent University, Ghent, Belgium
Email: Brecht.DeBeelde@UGent.be

***Abstract*—This paper presents a study on the joint antenna and channel modelling for communication in metallic kitchen environments. It allows characterizing and optimizing the wireless communication between the cooking pot and the kitchen hood in a smart kitchen where data acquired by sensors in the pot is used to control the kitchen hob and hood. The delay and path loss characteristics of the wireless channel are obtained from channel sounding measurements. The influence of the metallic pot on the antenna is taken into account by performing measurements with and without pot. The channel sounding measurements show a small delay spread caused by reflections on the hob and hood, and path loss values that are close to the free space path loss for a Line-of-Sight setup but up to 30 dB higher for different setups. The measurements with pot show lower losses, due to a more directive radiation pattern of the antenna when placed next to metal. Path loss and small scale fading margins are used for link budget calculations.**

***Index Terms*–channel characterization, modelling, path loss, channel sounding, kitchen environment, link budget**

I. Introduction

In the last decade, an increasing number of devices is connected to the internet, forming a global network of interconnected objects known as the Internet-of-Things (IoT) [1]. An important domain of IoT is the smart home, which consists of a network of devices providing electronics, sensors, software and connectivity inside the home [2], [3]. One part of the smart home is the smart kitchen where input from sensors in the kitchen hob, pots/pans and kitchen hood can support the cook during the cooking process, e.g. by automatically adjusting the hob and hood. Next to the smart kitchen's sensor and actuator capabilities, it can include a recipe recommendation system (e.g. as proposed in [4]). The architecture of this envisioned smart kitchen is displayed in Figure 1. This connected cooking system will improve the cooking experience and will lead to better meals with reduced chances of burnt, undercooked or overdone food.

An indispensable part of such a smart kitchen is a reliable wireless communication link. This is required to gather the sensor data in the kitchen controller (which is integrated in the hood). The radio channel depends on the kitchen environment defined by the presence of multiple metallic objects such as the kitchen hob, hood and pots. The metallic kitchen equipment introduces reflections of the electromagnetic waves and it influences the radiation pattern and efficiency of the antenna. The reflections of the transmitted signal are causing multipath propagation. In [5], multipath propagation characteristics are obtained via broadband channel modelling. This is done in metallic environments in [6], [7]. Path loss, i.e. the signal attenuation between transmit and receive antenna, has already been modelled in metallic environments in [8].

The goal of this paper is to characterize the wireless channel in a kitchen environment, with the purpose of optimizing the wireless communication between the pot and kitchen hood and accounting for the antenna properties near the metallic pot. Via this wireless link, the pot can send sensor data such as temperature and content level to the kitchen controller.

To the best of the authors' knowledge, this is the first time that the radio channel in a kitchen environment is modelled. The novelty of this paper is the joint antenna and channel modelling near metal and the calculation of the link budget. The influence of metal on the antenna is characterized by comparing measurements with and without pot.

The outline of the paper is as follows. In Section II we provide a methodology description. The results are presented in Section III and the conclusions and future work are discussed in Section IV.

II. Method

In the kitchen environment, multipath components (MPCs) will arise because different signal paths between the transmitter and receiver have a different length. This causes a pulse to spread in time. Therefore, we will investigate the power delay profile (PDP) [9] and path loss (PL). We characterize the radio channel via an empirical approach by using an ultra wide band (UWB) channel sounder.

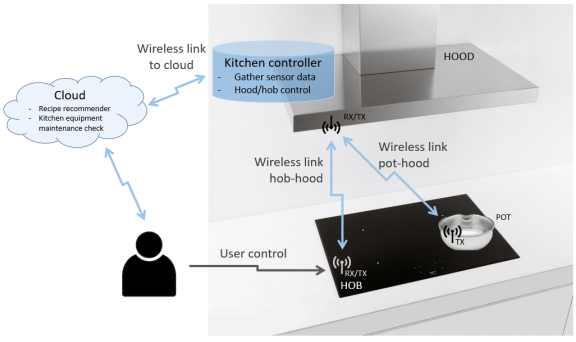

Fig. 1. Architecture overview of the envisioned smart kitchen

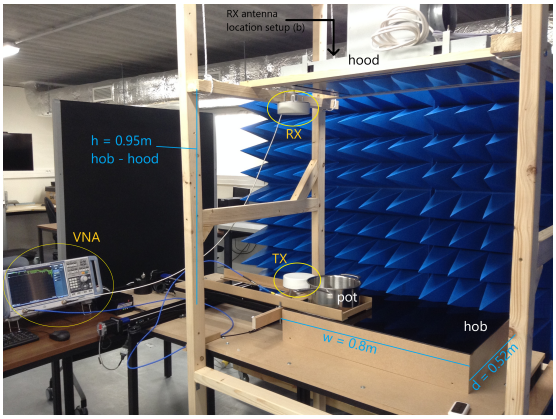

(a) Radio channel sounding measurement environment

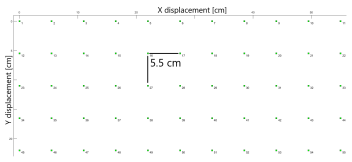

(b) URA grid

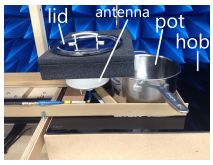

(c) TX antenna location

Fig. 2. Kitchen environment for channel sounding procedure

The channel is probed via a vector network analyzer (VNA) that feeds a signal to the transmitting antenna and analyzes the signal obtained by the receiving antenna.

A. Kitchen environment

Figure 2a shows the kitchen environment in which the experiments were performed. It consists of a hob and hood made of stainless steel. The height of the hood is fixed at 1.85 m, which is 0.95 m above the hob and 0.85 m below the ceiling. Absorbing cones are placed next to the setup to limit the influence of the room. The transmit (TX) antenna moves on a uniform rectangular array (URA) grid on the kitchen hob in order to characterize small scale fading (SSF) effects. The URA with a grid spacing of 5.5 cm is displayed in Figure 2b.

We consider two scenarios. In a first scenario, no pot is present on the hob. In the second scenario there is one pot present, made of stainless steel and with a diameter of 24 cm. For both scenarios we will investigate the following setups, using different receiver (RX) antenna locations:

(a) RX next to hood, Line-of-Sight (LOS), shown in Fig. 2a
(b) RX on top of hood, Non Line-of-Sight (NLOS)
(c) RX next to hood, TX covered by lid (during cooking) Obstructed Line-of-Sight (OBS), shown in Fig. 2c
(d) RX next to hob with TX antenna directed towards hob

These setups are schematically displayed in Figure 3.

B. Channel Measurement setup

The measurement setup for the radio channel sounding procedure consists of a VNA type Rohde & Schwarz ZNB20 and two directional broadband antennas type Cobham PSA operating in frequency range 500 MHz - 8 GHz. The VNA triggers a frequency sweep from 500 MHz up to 8 GHz,

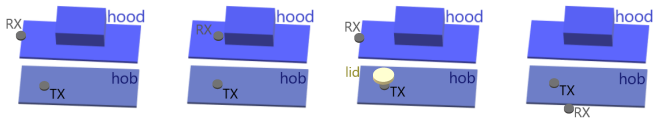

(a) LOS (b) NLOS (c) OBS (d) pot-hob

Fig. 3. Considered setups displayed for scenario 1

which yields a measurement bandwidth of 7.5 GHz or a time resolution of 0.13 ns. We use 2001 frequency points which gives a frequency inter spacing of 3.750 MHz that corresponds to a maximum resolvable time delay of 266 ns.

This channel sounding procedure results in a complex transfer function $H(f)$. After applying a Hann window to suppress side lobes, the inverse discrete Fourier transform (IDFT) gives the channel impulse response (CIR). The power delay profile (PDP) is found by taking the square of the CIR's amplitude. SSF effects are eliminated by spatial averaging on a URA to obtain a virtual antenna array, resulting in an averaged PDP (APDP). At each of the 55 locations of the URA, 10 frequency sweeps are performed. From the channel sounding procedure we obtain the following averaged path loss (PL), with the average taken over all 55 locations $\mathbf{r_j}$ of the URA and 10 observations t_k, and N the number of frequency points f_i in the frequency band with bandwidth B for which the path loss is calculated.

$$PL_{dB} = 10 \cdot log_{10}\left(\frac{1}{10 \cdot 55 \cdot N}\sum_{k=1}^{10}\sum_{j=1}^{55}\sum_{i=1}^{N}|H(f_i, \mathbf{r_j}, t_k)|^2\right) \quad (1)$$

We compare the measured PL to the free space path loss PL_0 calculated as follows, with c the speed of light (in m/s) and d_{avg} the average distance (in m) between the TX and RX antenna, averaged over the URA grid.

$$PL_{0,dB} = 20 \cdot log_{10}\left(\frac{4\pi d_{avg}}{c}\right) + 10 \cdot log_{10}\left(\frac{1}{B}\int_B f^2 df\right) \quad (2)$$

C. Metal influence on antenna

The antenna characteristics of the transmitting antenna will be altered when the antenna is placed next to the metallic pot. To account for the presence of metal we perform the same measurements for the two scenarios mentioned in Section II-A, scenario 1 without pot and scenario 2 where the TX antenna is placed next to the pot, as shown in Figure 2.

D. Joint antenna and channel modelling

We start by analyzing the APDP for the different setups. We then compare the averaged PL values of the two scenarios at different frequency bands and setups. The averaged PL values are used for link budget calculations, together with the receiver sensitivity and SSF margin.

Apart from the delay dispersion and averaged path loss values, we also compare the spatial variation of the path loss values on the URA for the two scenarios in order to characterize the pot influence on the TX antenna.

TABLE I
PATH LOSS AND STANDARD DEVIATION FOR SCENARIO 1 (WITHOUT POT) AND 2 (WITH POT)

Setup	868MHz				2.45GHz				5.0GHz			
	scenario 1		scenario 2		scenario 1		scenario 2		scenario 1		scenario 2	
	PL[dB]	σ[dB]	PL[dB]	σ[dB]	PL[dB]	σ[dB]	PL[dB]	σ[dB]	PL[dB]	σ[dB]	PL[dB]	σ[dB]
(a) LOS	30.0	1.6	28.6	1.1	31.8	3.4	28.7	2.8	39.6	1.1	38.0	2.4
(b) NLOS	57.6	1.7	60.8	4.1	64.8	2.7	60.0	3.1	72.5	1.7	69.1	3.1
(c) OBS	43.2	1.4	37.9	1.6	43.8	3.9	41.9	2.7	50.3	3.8	46.5	2.8
(d) hob-pot	46.5	5.2	38.8	6.8	42.4	4.7	40.3	4.1	57.0	3.4	48.8	3.9

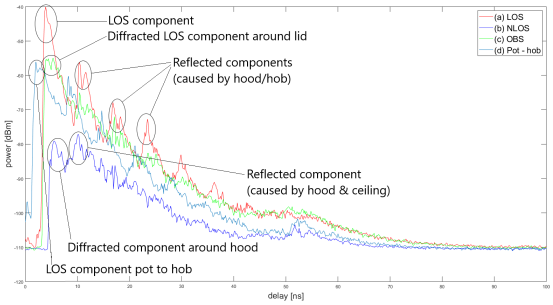

Fig. 4. Averaged Power Delay Profile (APDP), scenario 1

III. RESULTS

A. Delay dispersion

The delay spread causes inter symbol interference (ISI) and will be investigated by creating the APDP of the radio channel, as described in Section II-B. Figure 4 shows the APDP for scenario 2 (with pot) for the different setups explained in Section II-A.

Even though the maximum resolvable time delay is 266 ns, the APDPs are cut off at 100 ns as no energy higher than the noise threshold of -110 dBm is detected afterwards. From the APDPs we conclude that for setup (a) where the RX antenna is placed next to the hood, the received signal consists of the LOS component as well as reflections on the hob and hood. The spacing between power peaks is 6.6 ns, which corresponds to a round-trip distance of 1.9 m. Having multiple pots on the hob doesn't influence the APDP. In setup (b) the RX antenna is placed on top of the hood and the LOS component is diffracted. This causes an attenuation of 39 dB compared to the LOS component of setup (a). The same attenuation is encountered in setup (d) because the hob obstructs the LOS path between TX and RX antenna. Diffraction also causes a 15 dB attenuation in the LOS component of setup (c).

Examples of technologies that are suitable to be used in a smart kitchen environment are Bluetooth Low Energy (BLE) and IEEE 802.15.4 with a respective symbol time of 1 μs and 16 μs. From the APDP we can conclude that the maximum delay spread, i.e. the time between the first and last signal component with a power level above a certain threshold, is well below one-tenth of these symbol times.

B. Path loss

The averaged PL values and standard deviation of the spatial variation for three frequency bands and different setups are displayed in Table I. The measured PL values comprise the signal attenuation due to free space path loss as well as the combined TX and RX antenna gain and channel attenuation caused by the environment. The free space path loss averaged over the URA grid is 33 dB for the 868 MHz frequency band, 39 dB for the 2.4 GHz band and 45 dB for the 5.0 GHz band. Accounting for the antenna gain of 1 dB for the 868 MHz band and 5 dB for the 2.4 GHz and 5.0 GHz bands we conclude that the measured PL is close to the free space PL for setup (a) where there is a strong LOS component.

Table I shows that the link pot-hood is favorable over the link pot-hob, as in setup (d), the LOS component is obstructed by the hob and the PL depends more on the pot placement than for the link pot-hood, causing a higher standard deviation.

For the link pot-hood, the PL lowers with 1.5 to 5.3 dB when the TX antenna is placed next to the pot. The pot is placed at the right side of the TX antenna, whereas the RX antenna is placed at the left side of the hood. The lower losses are obtained by the presence of metal, making the TX antenna more directive in the direction of the RX antenna. This can also be seen by looking at the spatial variation of the PL on the URA grid. The spatial variation of the temporally averaged PL for the 2.4 GHz frequency band in setup (a) for both scenarios is displayed in Figure 5. The lowest PL value for scenario 1 is obtained when the TX antenna is right below the RX antenna. For scenario 2, the radiation pattern encounters a 10° beam tilt compared to scenario 1.

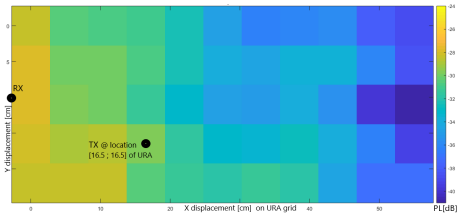

(a) Scenario 1 (w/o pot)

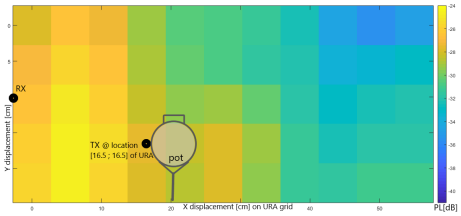

(b) Scenario 2 (w/ pot)

Fig. 5. Spatial variation of averaged path loss, LOS setup (a), 2.4 GHz

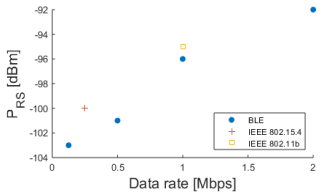

Fig. 6. Receiver Sensitivity P_{RS} as a function of data rate

TABLE II
SSF MARGIN BASED ON WORST CASE PL

Scenario	Setup	868 MHz	2.45 GHz	5.0 GHz
1	(a)LOS	4.3 dB	9.1 dB	5.4 dB
	(c)OBS	3.0 dB	13.0 dB	11.8 dB
2	(a)LOS	2.5 dB	6.9 dB	4.9 dB
	(c)OBS	3.9 dB	8.4 dB	7.7 dB

C. Joint channel and radiation pattern model for link budget calculation

Based on the PL values in Table I, the link budget is calculated as in Equation 3 in order to obtain the minimum transmit power P_T needed to allow wireless communication in our smart kitchen environment.

$$PL_{max} = P_T + G_T + G_R - L_T - L_R - P_{RS} \qquad (3)$$

For the remainder of this paper, we include the antenna gain in the PL so the antenna gains G_T of the TX and G_R of the RX antenna, as well as the feeder losses L_T and L_R in Equation 3 are assumed to be zero. The receiver sensitivity P_{RS}, i.e. the lowest signal power level at which the radio can reliably receive data, depends on the technology and data rate. The receiver sensitivity for different technologies and data rates is displayed in Figure 6.

In addition to the PL and receiver sensitivity in Equation 3, we take the SSF margin by subtracting the averaged PL from the highest PL value on the URA.

To get the minimum required TX power we use the averaged path loss values from Table I with the OBS setup as worst case scenario during the cooking process. We add the RX sensitivity for a BLE controller and SSF margin, which results in the TX powers displayed in Figure 7. The corresponding TX power is close to the minimum TX power of -40 dBm for a typical IEEE 802.15.4 or BLE communications controller.

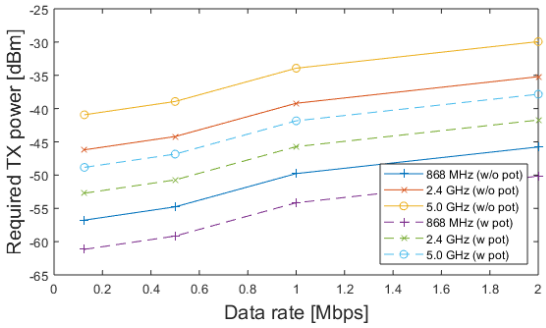

Fig. 7. Minimum TX power for different scenarios as a function of data rate

IV. CONCLUSIONS AND FUTURE RESEARCH

In this paper the radio channel characteristics of a kitchen environment have been studied, accounting for the influence of the metal pot on the antenna characteristics. The best wireless link is obtained with a Line-of-Sight configuration between the pot and the hood. By placing the antenna near the metallic pot, the directivity of the antenna increases.

Besides the path loss values and SSF margins, we take into account the receiver sensitivity to obtain a generic model with minimum required transmit power which can be used when designing a smart kitchen.

Future research includes extending the channel model with a Power Angular Profile (PAP) and measuring the actual radiation pattern of the antenna in an anechoic chamber when the antenna is placed next to the metallic pot. Combining the PAP and radiation pattern gives an exact antenna gain that can be accounted for in the link budget.

In addition to the extended channel model, a narrowband antenna will be designed that operates in the 2.4 GHz frequency band and can be integrated in the pot. The antenna will be modelled via Finite Difference Time Domain (FDTD) simulations and the measurement data will be used to validate our model.

ACKNOWLEDGMENT

This work was executed within the IoT Chef research project and EOS project MULti-Service WIreless NETwork MUSE-WINET. IoT Chef is co-financed by imec and received support from Flanders Innovation & Entrepeneurship.

REFERENCES

[1] D. Miorandi, S. Sicari, F. De Pellegrini, and I. Chlamtac, "Internet of things: Vision, applications and research challenges," *Ad Hoc Networks*, vol. 10, no. 7, pp. 1497–1516, sep 2012.

[2] M. Alaa, A. Zaidan, B. Zaidan, M. Talal, and M. Kiah, "A review of smart home applications based on Internet of Things," *Journal of Network and Computer Applications*, vol. 97, pp. 48–65, nov 2017.

[3] P. P. Gaikwad, J. P. Gabhane, and S. S. Golait, "A survey based on Smart Homes system using Internet-of-Things," in *2015 International Conference on Computation of Power, Energy, Information and Communication (ICCPEIC)*. IEEE, apr 2015, pp. 0330–0335.

[4] S. Sasirekha, I. J. L. Paul, and S. Swamynathan, "An API Centric Smart Kitchen Application," in *2018 International Conference on Computer, Communication, and Signal Processing*. IEEE, feb 2018, pp. 1–6.

[5] A. F. Molisch, K. Balakrishnan, C.-C. Chong, S. Emami, A. Fort, J. Karedal, J. Kunisch, H. Schantz, U. Schuster, K. Siwiak, Q.-T. U. Schuster, and E. Zurich, "IEEE 802.15.4a channel model-final report," Tech. Rep.

[6] J. Karedal, A. Singh, F. Tufvesson, and A. Molisch, "Characterization of a Computer Board-to-Board Ultra-Wideband Channel," *IEEE Communications Letters*, vol. 11, no. 6, pp. 468–470, jun 2007.

[7] E. Tanghe, D. P. Gaillot, M. Lienard, L. Martens, and W. Joseph, "Experimental Analysis of Dense Multipath Components in an Industrial Environment," *IEEE Transactions on Antennas and Propagation*, vol. 62, no. 7, pp. 3797–3805, jul 2014.

[8] R. J. Katulski, J. Sadowski, and J. Stefanski, "Propagation Path Loss Modeling in Container Terminal Environment," in *Proceedings of the 68th {IEEE} Vehicular Technology Conference, {VTC} Fall 2008, 21-24 September 2008, Calgary, Alberta, Canada*, sep 2008, pp. 1–4.

[9] E. Tanghe, D. P. Gaillot, D. Plets, W. Joseph, M. Liénard, W. De Ketelaere, and L. Martens, "Capacity analysis of an IEEE 802.11n system in a residential house based on estimated specular and dense multipath components," *IET Microwaves, Antennas & Propagation*, vol. 11, no. 12, pp. 1671–1675, sep 2017.